Study of pre-treatment of quinoline in aqueous solution using activated carbon made from low-cost agricultural waste (walnut shells) modified with ammonium persulfate

Tao Yang, Xuansheng Hu, Peijuan Zhang, Xiaogang Chen, Weiwei Wang, Yanping Wang, Qiuxia Liang, Yingjiu Zhang and Qunce Huang

ABSTRACT

Activated carbon made from agricultural waste (walnut shells) was investigated as a suitable adsorbent for effectively removing quinoline from industrial wastewater. The activated carbon was treated with phosphoric acid and oxidized by ammonium persulfate and its ability to adsorb pyridine and quinoline in aqueous solution was investigated. Kinetic parameters for the adsorption process were determined through pseudo-first-order and pseudo-second-order kinetic models and intraparticle diffusion models. Equilibrium experiments and adsorption isotherms were analyzed using Langmuir and Freundlich adsorption isotherms. After reaching equilibrium, the activated carbon adsorbed quinoline in preference to pyridine: the equilibrium adsorptions from individual aqueous solutions ($200 \, \mu L \, L^{-1}$) of quinoline and pyridine were $166.907 \, mg \, g^{-1}$ and $72.165 \, mg \, g^{-1}$, respectively. Thermodynamic studies of quinoline adsorption were conducted at different temperatures and indicated that quinoline adsorption was an endothermic and spontaneous process. The column-adsorption of quinoline and pyridine was consistent with the Thomas model and the Yoon-Nelson model. The removal efficiency of quinoline reached more than 97% for a velocity of $6 \, mL \, min^{-1}$ at the initial adsorption stage.

Key words | activated carbon, ammonium persulfate oxidation, column-adsorption process, equilibrium studies, kinetic parameters, quinoline

Tao Yang
Peijuan Zhang (corresponding author)
Weiwei Wang
Yanping Wang
Qiuxia Liang
Qunce Huang
Henan Provincial Key Laboratory of Ion Beam Bioengineering, School of Physics and Engineering,
Zhengzhou University,
Zhengzhou 450052,
China
E-mail: zhangpeijuan@yeah.net

Tao Yang
Xiaogang Chen
Yingjiu Zhang
Key Laboratory of Materials Physics of Ministry of Education, School of Physics and Engineering,
Zhengzhou University,
Zhengzhou 450052,
China

Xuansheng Hu
College of Biology Pharmacy and Food Engineering,
Shangluo University,
Shangluo 726000,
China

INTRODUCTION

Removal of nitrogen heterocyclic compounds (NHCs), which are generated ubiquitously by coking plants, pharmaceutical factories, and related industries, has been extensively studied because of their high priority as environmental contaminants with toxic, carcinogenic and teratogenic properties (Shi *et al.* 2019). Due to the low biodegradability, the malodorous compound quinoline, as a typical example of an NHC, can be stable in water and soil for long periods of time (Lu *et al.* 2019). Consequently, it is essential that it is removed from wastewater before it is discharged into the environment.

Quinoline cannot be readily removed by conventional water treatment methods; therefore advanced treatment processes are required, such as microbiological degradation (Liu *et al.* 2016; Dinamarca *et al.* 2018), physico-chemical adsorption (Rameshraja & Srivastava 2012), catalytic degradation (Chang *et al.* 2014; Lovjeet *et al.* 2018) and biosorption–adsorption of clay minerals or activated carbon with attached microorganisms (Bai *et al.* 2010; Buchtmann *et al.* 2015). Among these, the method of immobilization of quinoline-degrading bacteria on different sorption carriers is an environmentally friendly alternative to achieve complete removal of contaminants. Accordingly, the choice of the sorption carriers will play an indispensable and important role.

The main disadvantage of taking clay mineral materials as sorption carriers, such as zeolite, bentonite and montmorillonite, is that competitive interactions of monovalent

cations, in particular Na⁺ and K⁺, can significantly block the adsorption of NHCs. It has been found that in ion exchange processes, inorganic ions are easier to exchange than organic ions (Ding et al. 2013).

Activated carbon has been used as a biofilm carrier, whose role in the physical adsorption in association with biodegradation was proved in the wastewater process (Scott & Karanjkar 1998; Klimenko et al. 2002). The attached microorganisms breed faster with an increased metabolic activity.

In the present study, low-cost biosorbents for quinoline in water were prepared from walnut shells derived from agricultural waste. The process involved converting the walnut shells into activated carbon, using phosphoric acid as an activating agent, and modification by ammonium persulfate oxidation. The focus of the work was to understand the properties of the activated carbon adsorbent in the absence of a biofilm. The ability of the activated carbon to adsorb quinoline in aqueous solution was investigated with individual solutions of quinoline and pyridine, and with a mixture of the two, in kinetic, equilibrium, thermodynamic and column-adsorption studies.

MATERIALS AND METHODS

Preparation of high-performance walnut shell activated carbon adsorbent

Walnut shells were obtained from a local market. Walnut shell activated carbon was prepared by treatment of the shells with phosphoric acid followed by mild oxidation (Lim et al. 2010; Li et al. 2011). First, the walnut shells were boiled to remove impurities, oven-dried, crushed, and sieved to a particle size of 0.3–0.5 mm. Next, the shells were mixed with 60% phosphoric acid (1:2.5 w/w) and maintained at 60 °C for 48 h. The shells were then carbonized for 80 min at 300 °C and then activated for 80 min at 600 °C in an SX2-4-13 type muffle furnace. The activated carbon obtained was thoroughly washed with 0.1 M hydrochloric acid and distilled water and dried at 105 °C for 24 h. Finally, the resulting activated carbon was oxidized by mixing 1.0 g of walnut shell activated carbon (WSAC) with 20 mL of a 2.0 mol L⁻¹ solution of ammonium persulfate, $(NH_4)_2S_2O_8$, in a glass conical flask and keeping it at 60 °C for 3 h. The oxidized material was filtered, washed with the distilled water, dried in a vacuum oven at 110 °C for 24 h, and then sealed in a vial before use. The oxidized WSAC samples were denoted as OWSAC.

Adsorption kinetic studies of the OWSAC surface

OWSAC (0.1 g) was added to a 100 mL aqueous solution containing 200 μL L⁻¹ of either pyridine, quinoline or a mixture of the two (pyridine:quinoline = 2:3 v/v) in a 250 mL glass flask. The three flasks were shaken simultaneously at the room temperature by a double shaker (TAITEC NR-30, Japan) at 160 rpm for 600 min. Samples of the supernatant (about 0.5 mL) were withdrawn at regular intervals to determine the concentration of the pyridine and/or quinoline. In order to investigate the mechanism of adsorption, data were fitted to Lagergren's pseudo-first-order kinetic model (Karamanis & Assimakopoulos 2007) and pseudo-second-order kinetic model (Parab & Sudersanan 2010) and analyzed with the intraparticle diffusion equation.

Lagergren's pseudo-first-order kinetic model:

$$q_t = q_e(1 - e^{-k_1 t})$$

and pseudo-second-order kinetic model:

$$q_t = \frac{k_2 q_e t}{1 + k_2 q_e t}$$

where t (min) is the contact time, k_1 (min⁻¹) and k_2 (g mg⁻¹ min⁻¹) are the adsorption rate constants, and q_e and q_t (mg g⁻¹) represent the uptake amount of pyridine or quinoline by the adsorbent at equilibrium and time t, respectively.

The limiting step of the adsorption process can be predicting from the diffusion coefficient using a diffusion-based model. The possibility of intraparticle diffusion resistance affecting the adsorption was explored in this study by using the intraparticle diffusion equation (Delchet et al. 2012):

$$q_t = K_t t^{1/2} + C$$

where t (min) is the contact time, q_t (mg g⁻¹) is the quinoline or pyridine uptake amount at time t, K_t (mg g⁻¹ min⁻¹/²) is the intraparticle diffusion rate constant and can be determined from the slopes of linear plots, and C is a constant that indicates the thickness of the boundary layer, i.e. the larger the value of C the greater is the boundary layer effect.

Equilibrium studies and adsorption isotherms

A series of experiments were carried out with different concentrations of either pyridine, quinoline or a mixture of the two (pyridine:quinoline = 2:3 v/v). Ten different volumes of

NHC were used (5 μL increments in the range 5–50 μL). For each volume, the NHC was added to 100 mL of water and 0.1 g of OWSAC in a 250 mL Erlenmeyer flask and the three flasks shaken at 160 rpm. After 12 h the resultant supernatants were withdrawn and the concentration of the NHCs determined.

It was important to establish the most appropriate correlation for the equilibrium adsorption state. The Langmuir and Freundlich adsorption isotherms were used to fit the experimental adsorption results (Ding *et al.* 2013). The non-linear forms of these isotherms are given as follows.

Langmuir isotherm:

$$q_e = \frac{q_m K_L C_e}{1 + K_L C_e}$$

Freundlich isotherm:

$$q_e = K_F C_e^{1/n}$$

where q_e (mg g^{-1}) is the amount of NHC adsorbed at equilibrium, C_e (mg L^{-1}) is the equilibrium concentration of NHC. K_L (L mg^{-1}) is a constant related to the free energy or net enthalpy of adsorption ($K_L \propto e^{-\Delta G/RT}$) and q_m (mg g^{-1}) is the adsorption capacity at the isotherm temperature. K_F and n are equilibrium constants indicative of adsorption capacity and adsorption intensity, respectively.

Thermodynamic studies

OWSAC (0.01 g) was added to 10 mL of an aqueous solution containing 50 μL L^{-1} of either pyridine, quinoline or a mixture of the two (pyridine:quinoline 2:3 v/v) at one of three different temperatures (293, 303, and 313 K) and the temperature maintained for 24 h. Three thermodynamic parameters – standard Gibbs free energy (ΔG^o), standard enthalpy (ΔH^o) and standard entropy (ΔS^o) changes – were determined in order to investigate the thermodynamic nature of the adsorption process. The quantities ΔH^o and ΔS^o were calculated from the slope and intercept, respectively, of the straight line obtained from plotting lnK_d versus $1/T$ using the following equation (Mohan & Singh 2002):

$$\ln K_d = \frac{\Delta S^o}{R} - \frac{\Delta H^o}{RT}$$

where K_d (mL g^{-1}) is the distribution coefficient, R (8.314 J mol^{-1} K^{-1}) is the gas constant and T (K) is the absolute temperature of the aqueous solution.

After obtaining ΔH^o and ΔS^o values for the adsorption, ΔG^o at each temperature was calculated using the well-known equation:

$$\Delta G^o = \Delta H^o - T\Delta S^o$$

Column adsorption model

In order to improve efficiency, practical wastewater treatment usually uses a column packed with adsorbent. Therefore, it was imperative to investigate the dynamic adsorption of quinoline by OWSAC in a packed column. In this study, Thomas and Yoon-Nelson models were employed to estimate the quinoline adsorption efficiency with different velocities of an aqueous solution (200 μL L^{-1}) from a mixture solution (pyridine:quinoline 2:3 v/v). Experiments used 2.5 g of OWSAC and a column with diameter 1.2 cm and height 4.5 cm.

The theoretical models were defined as follows.

Thomas model:

$$\frac{C_t}{C_0} = \frac{1}{1 + \exp\left((K_{th} q_0 x / v) - K_{th} C_0 t\right)}$$

Yoon-Nelson model:

$$\frac{C_t}{C_0} = \frac{1}{1 + \exp\left[k(\tau - t)\right]}$$

where K_{th} is the Thomas velocity constant (mL min^{-1} mg^{-1}); q_0 is the adsorbance per unit mass of adsorbent to adsorbate at equilibrium (mg g^{-1}); x is adsorbent quantity used to fill the column (g); C_0 is the initial concentration of adsorbate (mg L^{-1}); C_t is the effluent concentration of adsorbate (mg L^{-1}); v is the velocity of the adsorbate through the column (mL min^{-1}); k is the velocity constant (min^{-1}); τ is time needed for 50% of the adsorbate to be adsorbed (min); and t is time of adsorption.

Analysis

In order to ensure reliability and improve accuracy of the experimental data in this study, static and mobile adsorption of pyridine and quinoline were investigated in duplicate and the mean standard deviation determined. All samples were collected by filtering the supernatant through a 0.22 μm mixed cellulose ester membrane (Millipore, Ireland). The filtered supernatant was then analyzed with a double beam visible spectrophotometer (RUNQEE G10, China) and

reverse phase high-pressure liquid chromatography (HPLC, ichrom5100, China), using a C18 column (250 mm length and 4.6 mm internal diameter) and UV detection at 254 and 275 nm. The mobile phase consisted of methanol and water in the ratio 75:25 v/v with a flow rate of 1 mL min^{-1}. All of the figures and the data fitting presented in this paper were obtained using the Origin 7.5 program (OriginLab, USA).
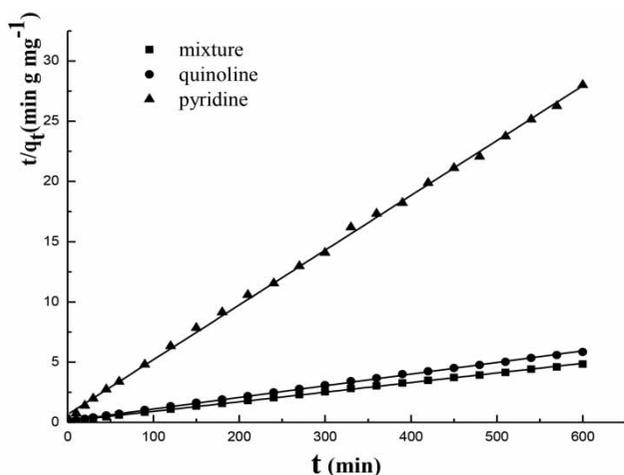

Figure 1 | The pseudo-second-order kinetic curve of individual solutions of quinoline and pyridine, and a mixed solution of the two: OWSAC (0.1 g) added to a 100 mL aqueous solution containing 200 μL L^{-1} of either pyridine, quinoline or a mixture of the two (pyridine:quinoline = 2:3 v/v) in a 250 mL glass flask at room temperature under 160 rpm shaking, detected by spectrophotometer and HPLC.

RESULTS AND DISCUSSION

The adsorption process and kinetic study

The adsorption mechanism of quinoline and pyridine by OWSAC was investigated by using dynamic adsorption models of pseudo-first-order kinetics, pseudo-second-order kinetics, and intraparticle diffusion. Fitting the experimental data for quinoline and pyridine showed that the adsorption processes were more consistent with pseudo-second-order kinetics rather than pseudo-first-order kinetics (see Table 1 and Figure 1). This finding indicated that the adsorption processes tended to involve chemical reaction accompanied by physical adsorption (Aksu 2002). After 60 minutes, the equilibrium adsorptions of individual solutions of quinoline and pyridine by OWSAC were 166.9 and 72.2 mg g^{-1} respectively. This suggested that the OWSAC adsorbed quinoline more readily than pyridine in aqueous solution. The corresponding total adsorption from a mixed solution of quinoline and pyridine was 124.29 mg g^{-1}; the individual absorbances of quinoline and pyridine from the mixed solution were 98.6 and 26.75 mg g^{-1} respectively. The adsorption of quinoline was about 2.5 times that of pyridine. This indicated that there was no significant difference in the adsorptions of quinoline and pyridine by OWSAC in the individual and mixed solutions.

The above results show that the adsorption property of OWSAC for quinoline displayed a stronger advantage than

Table 1 | The sorption rate constants associated with pseudo-first- and pseudo-second-order kinetic and intraparticle diffusion models from individual solutions of quinoline and pyridine, and a mixed solution of the two: OWSAC (0.1 g) added to a 100 mL aqueous solution containing 200 μL L^{-1} of either pyridine, quinoline or a mixture of the two (pyridine:quinoline = 2:3 v/v) in a 250 mL glass flask at room temperature under 160 rpm shaking, detected by spectrophotometer and HPLC

Adsorption dynamic equations and parameters	Quinoline	Pyridine	Mixture of quinoline and pyridine (3:2)
Pseudo-first-order			
k_1 (min^{-1})	0.0064	0.0064	0.0076
q_e^{exp} (mg g^{-1})	166.907 ± 0.0658	72.1655 ± 0.0589	124.2910 ± 0.0784
q_e^{cal} (mg g^{-1})	25.7929 ± 0.0457	17.5914 ± 0.0279	37.446 ± 0.0368
R^2	0.9086	0.9829	0.9421
Pseudo-second-order kinetic model			
k_2 (g·mg^{-1} min^{-1})	0.0001	0.0014	0.0242
q_e^{exp} (mg g^{-1})	166.907 ± 0.075	72.1655 ± 0.0653	124.2910 ± 0.0358
q_e^{cal} (mg g^{-1})	166.667 ± 0.0684	72.4638 ± 0.0569	125 ± 0.0469
R^2	0.9998	0.9996	0.9992
Intraparticle diffusion			
K_{t1}	127.53	44.0076	44.4518
Pseudo-first-order	3.342	1.6	4.4043
Pseudo-first-order	0.6741	0.429	0.8835

that of a commercial-grade coconut-based granular activated carbon with a determined quinoline saturated adsorption capacity of $77.82 \ mg \ g^{-1}$ in an individual quinoline solution under the similar condition (Rameshraja & Srivastava 2012).

Figure 2 shows plots of q_t versus $t^{1/2}$ for the adsorption of individual solutions of quinoline and pyridine, and a mixed solution of the two, by OWSAC at room temperature. These plots showed similar trends, with each adsorption process containing three regions. None of the curves passed through the origin of coordinates for times between 2 and 120 minutes, which indicated that intraparticle diffusion was not the only controlling step for adsorption. Rather, it was the combination of surface adsorption and intraparticle transport within the pores of OWSAC that controlled the adsorption process.

The slope of the linear portion of the plots shown in Figure 2 is the rate constant K_t of intraparticle diffusion (Lorenc-Grabowska & Gryglewicz 2005). The slope increases with the adsorption rate, where K_{t1}, K_{t2}, and K_{t3} represent the diffusion rate constant for the three stages. The rate constant in the first stage (K_{t1}) was the biggest, which indicated that external diffusion adsorption was very fast. After saturating the outer surface of the adsorbent particles, quinoline and pyridine entered the inner pores of the OWSAC and were adsorbed by particles of the inner surface. Meanwhile, the diffusional resistance gradually increased as quinoline and pyridine diffused into the inner surface of the OWSAC, and the intraparticle diffusion speed decreased until it reached the adsorption equilibrium. Consequently, the rate constant in the second stage (K_{t2}) was smaller than in the first stage, and smallest of all in the third stage (K_{t3}).

Equilibrium studies and adsorption isotherms

In order to obtain the equilibrium isotherm, 1 g of adsorbant was used and the initial concentrations of NHC were varied from 50 to $500 \ \mu L \ L^{-1}$. In each case, the amounts of adsorbed quinoline and pyridine were determined.

Figure 3 shows the application of nonlinear Langmuir and Freundlich isotherms for the adsorption of quinoline and pyridine, from separate solutions, at 313 K. Figure 4 shows the quinoline adsorption for a mixed solution of quinoline and pyridine at 293, 303, and 313 K. It can be seen that the adsorption processes were in agreement with the Freundlich isotherm rather than Langmuir isotherm.

The values of the monolayer saturation capacity q_m, calculated from the Langmuir isotherm, were approximately $294 \ mg \ g^{-1}$ for both quinoline and pyridine adsorptions from separate solutions. This result shows superiority
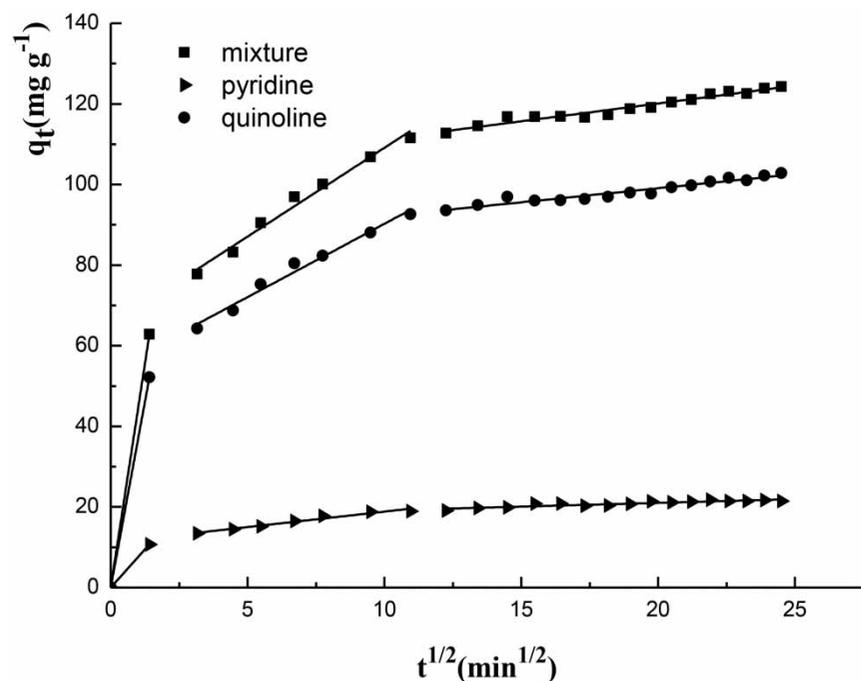

Figure 2 | Intraparticle diffusion model analysis of individual solutions of quinoline and pyridine, and a mixed solution of the two: OWSAC (0.1 g) added to a 100 mL aqueous solution containing $200 \ \mu L \ L^{-1}$ of either pyridine, quinoline or a mixture of the two (pyridine:quinoline = 2:3 v/v) in a 250 mL glass flask at room temperature under 160 rpm shaking, detected by spectrophotometer and HPLC.
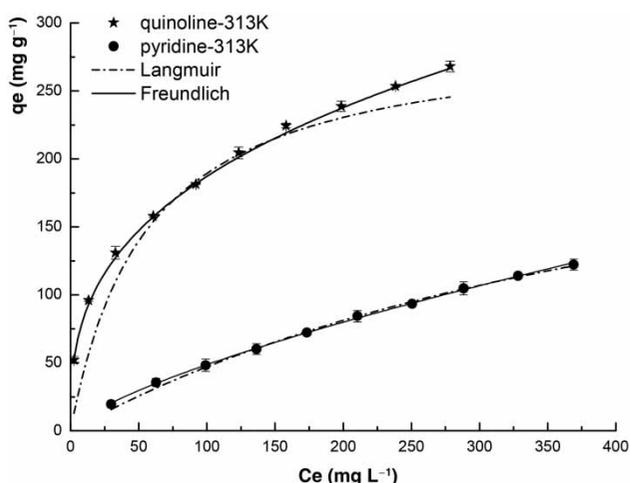
Figure 3 │ Nonlinear Langmuir (dashed line) and Freundlich (solid line) isotherms analysis of quinoline and pyridine adsorption, from separate solutions, shaken under 160 rpm at 313 K for 12 h: 1 g of adsorbant used and the initial concentrations of NHC varied from 50 to 500 μL L^{-1}. In each case, the amounts of adsorbed quinoline and pyridine were determined at 275 nm and 254 nm wavelength by spectrophotometer.
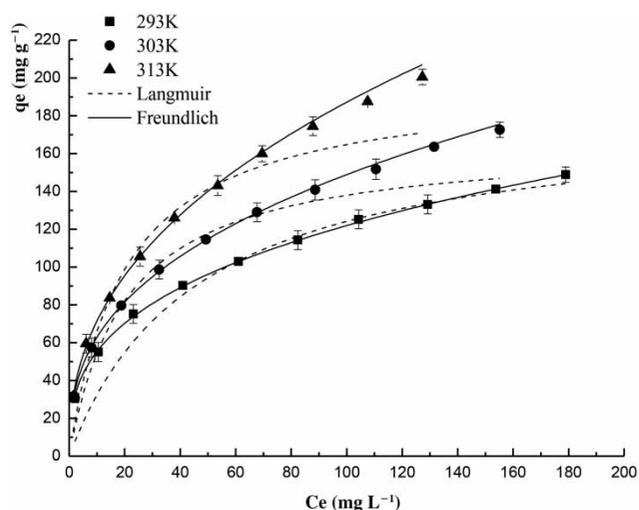

Figure 4 │ Nonlinear Langmuir (dashed line) and Freundlich (solid line) isotherms analysis of the quinoline adsorption for a mixed solution of quinoline and pyridine (pyridine:quinoline = 2:3 v/v) shaken at 293, 303, and 313 K for 12 h to reach adsorption equilibrium: 1 g of adsorbant used and the initial concentrations of NHC varied from 50 to 500 μL L^{-1}; then quinoline concentration was measured at 275 nm wavelength by HPLC.

compared with the maximum quinoline adsorption capacity of 56.6 mg g^{-1} obtained by the Langmuir model for the sulfuric acid-treated activated carbon from coconut shell (Ferreira *et al.* 2019).

Subsequently, in order to assess whether the two single adsorption processes were consistent with the Langmuir or the Freundlich isotherms, a chi-square analysis was used to estimate the degree of difference (χ^2) between the experimental and theoretical isotherms. The equation used for chi-square analysis (Mirmohseni *et al.* 2012) was:

$$\chi^2 = \sum \frac{(q_e^{exp} - q_e^{cal})^2}{q_e^{cal}}$$

where q_e^{cal} (mg g^{-1}) is the equilibrium uptake amount calculated from the isotherm and q_e^{exp} (mg g^{-1}) is the experimental equilibrium uptake. A smaller χ^2 value indicated a better fitting isotherm.

From Table 2, it is clear that not only were the r^2 values closer to unity for the Freundlich isotherm, but also the χ^2 values for the Freundlich isotherm were much smaller, implying that the individual adsorption processes of quinoline and pyridine on OWSAC were multilayer adsorption processes rather than monolayer adsorption.

Adsorption thermodynamic parameter

The thermodynamic parameters of quinoline adsorbed from an aqueous quinoline solution and from an aqueous solution of quinoline and pyridine (pyridine:quinoline = 2:3 v/v) are shown in Table 3. Similar thermodynamic parameters for quinoline adsorption were found for both solutions, indicating that the adsorption processes for quinoline were not affected by the presence of pyridine. The endothermic nature of the adsorption process was shown by the positive value of $\Delta H°$; however, increased randomness at the solid/solution interface, with some structural changes in the adsorbate and adsorbent system for quinoline, was indicated by the positive value of $\Delta S°$. The negative value of $\Delta G°$ suggested that the adsorption process was spontaneous.

Table 2 │ Langmuir and Freundlich adsorption isotherm constants analysis of individual solutions of quinoline and pyridine shaken under 160 rpm at 313 K for 12 h : 1 g of OWSAC used and the initial concentrations of the individual solution varied from 50 to 500 μL L^{-1}. In each case, the amounts of adsorbed quinoline and pyridine were determined at 275 nm and 254 nm wavelength by spectrophotometry respectively

		Quinoline	Pyridine
Langmuir	q_m(mg g^{-1})	294.4007 ± 0.5000	294.3438 ± 0.4000
	K_L	0.0180 ± 0.0048	0.0019 ± 0.0002
	R^2	0.8683	0.9961
	χ^2	152.0799	1.5533
Freundlich	K_F	38.0589 ± 0.42	1.8107 ± 0.48
	n	2.89 ± 0.039	1.399 ± 0.013
	R^2	0.9987	0.9995
	χ^2	0.4029	0.1263

Table 3 | Thermodynamic parameters for quinoline adsorption from individual quinoline solution and a mixture solution of quinoline and pyridine (pyridine:quinoline 2:3 v/v) onto OWSAC shaken at three different temperatures (293, 303, and 313 K) for 24 h ($C_{0individual}$ = 54.65 mg L^{-1}, C_{0mixed} = 32.79 mg L^{-1}, m_{OWSAC} = 1 g L^{-1})

	K_d (L g^{-1})		$\Delta G°$ (kJ mol^{-1})		$\Delta H°$ (kJ mol^{-1})		$\Delta S°$ (J mol^{-1} K^{-1})	
T(K)	individual	mixed	individual	mixed	individual	mixed	individual	mixed
293	17.3824 ± 0.061	14.9912 ± 0.055	−6.9632 ± 0.054	−6.9513 ± 0.018	5.9612 ± 0.0537	14.1801 ± 0.026	44.0623 ± 0.034	71.0244 ± 0.037
303	18.7012 ± 0.052	18.8804 ± 0.061	−7.3847 ± 0.062	−7.0245 ± 0.028				
313	20.3125 ± 0.018	21.7636 ± 0.064	−7.8441 ± 0.057	−8.1536 ± 0.048				

Thomas and Yoon-Nelson models analysis of dynamic adsorption

In this study, the column-adsorption of quinoline and pyridine from a mixed solution (quinoline:pyridine = 3:2 v/v) with an initial concentration of 200 μL L^{-1} using 2.5 g of

OWSAC with column diameter 1.2 cm and height 4.5 cm was consistent with the Thomas and Yoon-Nelson models (Qu *et al.* 2019). Linear plots were obtained by plotting $\ln[C_0/(C_t − C_0)]$ and $\ln[C_t/(C_0 − C_t)]$ against t, according to the two models respectively (see Figure 5). Figure 6 shows that the removal efficiency of quinoline from the mixed solution decreased with an increase in time and velocity of flow.

The removal efficiency of quinoline reached more than 97% for a velocity of 6 mL min^{-1} and 93% for 8 mL min^{-1} in the initial adsorption stage. In contrast, the corresponding efficiencies for pyridine were much lower: approximately 65% and 58%, respectively (data not shown). Benefield *et al.* (1982) proposed the idea of dynamic adsorption, with saturated adsorption being reached when the concentration of adsorbate in the effluent was 0.95 times that of the import solution. In our study, it took about 6 h for quinoline adsorption to reach equilibrium at a velocity 8 mL min^{-1}; this was about 2.6 times the adsorption rate for pyridine. These findings suggested that OWSAC adsorbed quinoline more effectively than pyridine.
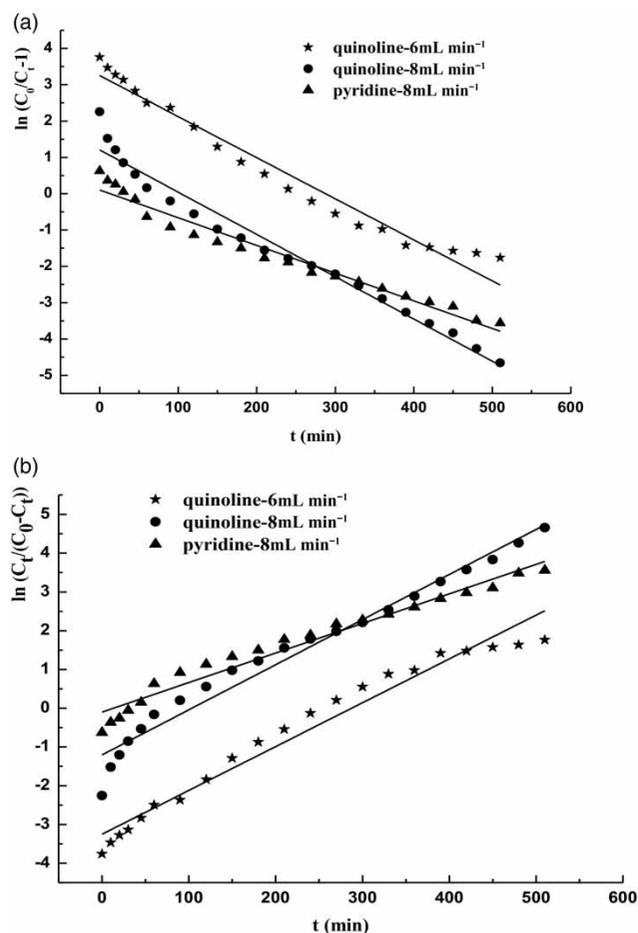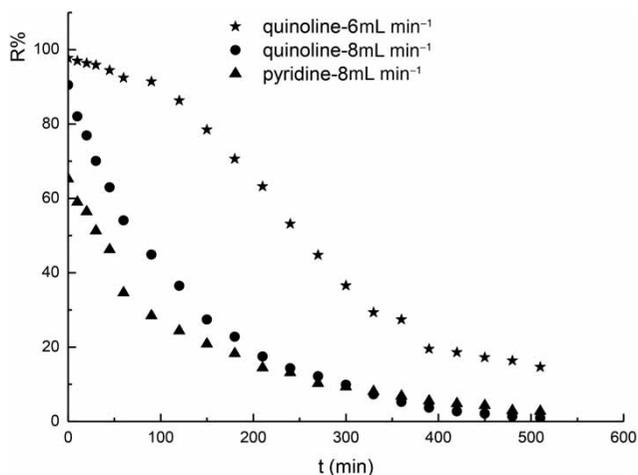

Figure 5 | (a) Thomas and (b) Yoon-Nelson models analysis of the quinoline adsorption with different velocities of an aqueous solution (200 μL L^{-1}) from a mixture solution (pyridine:quinoline 2:3 v/v). Experiments used 2.5 g of OWSAC and a column with diameter 1.2 cm and height 4.5 cm.

Figure 6 | The removal efficiency of quinoline and pyridine with different velocities of an aqueous solution (200 μL L^{-1}) from a mixture solution (pyridine:quinoline 2:3 v/v). Experiments used 2.5 g of OWSAC and a column with diameter 1.2 cm and height 4.5 cm.

CONCLUSION

In this study, OWSAC (prepared from walnut shells as agricultural waste, modified with a weak acid activator and a weak oxidizer) exhibited significant adsorption capacity for quinoline in aqueous solution in a physicochemical multilayer adsorption process. The rapid adsorption process fitted well with the pseudo-second-order kinetic model with the equilibrium uptake amount for quinoline and pyridine of 166.9 mg g^{-1} and 72.2 mg g^{-1} respectively. The good correlation coefficients with low χ^2 suggest that the adsorption of quinoline and pyridine on OWSAC could be best described by the Freundlich adsorption isotherm.

Intraparticle diffusion studies showed that the surface adsorption and intraparticle transport within the pores of OWSAC controlled the adsorption process. Thermodynamic parameters were evaluated using equilibrium constants determined at different temperatures. The value of ΔG° was found to be negative at all temperatures, indicating the spontaneity of the adsorption process. Positive values of ΔH° and ΔS° showed the endothermic nature and increase in disorder associated with quinoline adsorption. The column-adsorption process of quinoline and pyridine was consistent with the Thomas and Yoon-Nelson models. The removal efficiency of quinoline reached more than 97% for a velocity of 6 mL min^{-1}.

REFERENCES

Aksu, Z. 2002 Determination of the equilibrium, kinetic and thermodynamic parameters of the batch biosorption of nickel (II) ions onto *Chlorella vulgaris*. *Process Biochemistry* **38** (1), 89–99.

Bai, Y. H., Sun, Q. H., Xing, R., Wen, D. H. & Tang, X. Y. 2010 Removal of pyridine and quinoline by bio-zeolite composed of mixed degrading bacteria and modified zeolite. *Journal of Hazardous Materials* **181** (1), 916–922.

Benefield, L. D., Judkins, J. F. & Weand, B. L. 1982 *Process Chemistry for Water and Wastewater Treatment*. Prentice-Hall, Englewood Cliffs, NJ, USA.

Buchtmann, C., Kies, U., Deckwer, W. D. & Hecht, V. 2015 Performance of three phase fluidized bed reactor for quinoline degradation on various supports at steady state and dynamic conditions. *Biotechnology & Bioengineering* **56** (3), 295–303.

Chang, L., Zhang, Y. M., Gan, L., Xu, H., Yan, N., Liu, R. & Rittmann, B. E. 2014 Internal loop photo-biodegradation reactor used for accelerated quinoline degradation and mineralization. *Biodegradation* **25** (4), 587–594.

Delchet, C., Tokarev, A., Dumail, X., Toquer, G., Barre, Y., Guari, Y., Guerin, C., Larionova, J. & Grandjean, A. 2012 Extraction of radioactive cesium using innovative functionalized porous materials. *RSC Advances* **2** (13), 5707–5716.

Dinamarca, M. A., Eyzaguirre, J., Baeza, P., Aballay, P., Canales, C. & Ojeda, J. 2018 A new functional biofilm biocatalyst for the simultaneous removal of dibenzothiophene and quinoline using *Rhodococcus rhodochrous* and curli amyloid overproducer mutants derived from *Cobetia* sp. strain MM1IDA2H-1. *Biotechnology Reports* **20**, e00286.

Ding, D. H., Zhao, Y. X., Yang, S. J., Shi, W. S., Zhang, Z. Y., Lei, Z. F. & Yang, Y. N. 2013 Adsorption of cesium from aqueous solution using agricultural residue – walnut shell: equilibrium, kinetic and thermodynamic modeling studies. *Water Research* **47** (7), 2563–2571.

Ferreira, M. E. O., Vaz, B. G., Borba, C. E., Alonsoa, C. G. & Ostroski, I. C. 2019 Modified activated carbon as a promising adsorbent for quinoline removal. *Microporous and Mesoporous Materials* **277**, 208–216.

Karamanis, D. & Assimakopoulos, P. A. 2007 Efficiency of aluminum-pillared montmorillonite on the removal of cesium and copper from aqueous solutions. *Water Research* **41** (9), 1897–1906.

Klimenko, N., Winther-Nielsen, M., Smolin, S., Nevynna, L. & Sydorenko, J. 2002 Role of the physico-chemical factors in the purification process of water from surface-active matter by biosorption. *Water Research* **36**, 5132–5140.

Li, N., Ma, X. L., Kim, K., Chen, Y. S. & Song, C. S. 2011 Maximizing the number of oxygen-containing functional groups on activated carbon by using ammonium persulfate and improving the temperature-programmed desorption characterization of carbon surface chemistry. *Carbon* **49** (15), 5002–5013.

Lim, W. C., Srinivasakannan, C. & Balasubramanian, N. 2010 Activation of palm shells by phosphoric acid impregnation for high yielding activated carbon. *Journal of Analytical and Applied Pyrolysis* **88** (2), 181–186.

Liu, J., Yu, Y., Chang, Y., Li, B. K., Bian, D. J., Yang, W., Huo, H. L., Huo, M. X. & Zhu, S. Y. 2016 Enhancing quinoline and phenol removal by adding *Comamonas testosteroni* bdq06 in treatment of an accidental dye wastewater. *International Biodeterioration & Biodegradation* **115**, 72–84.

Lorenc-Grabowska, E. & Gryglewicz, G. 2005 Adsorption of lignite-derived humic acids on coal-based mesoporous activated carbons. *Journal of Colloid & Interface Science* **284** (2), 416–423.

Lovjeet, S., Pawan, R. & Shri, C. 2018 Comparative evaluation of synthesis routes of Cu/zeolite Y catalysts for catalytic wet peroxide oxidation of quinoline in fixed-bed reactor. *Journal of Environmental Management* **215**, 1–12.

Lu, Q. Y., Zhang, C. Y., Wang, W. Y., Yuan, B. Y., Zhang, Y. M. & Rittmann Bruce, E. 2019 Bioavailable electron donors leached from leaves accelerate biodegradation of pyridine and quinoline. *Science of the Total Environment* **654**, 473–479.

Mirmohseni, A., Seyed Dorraji, M. S., Figoli, A. & Tasselli, F. 2012 Chitosan hollow fibers as effective biosorbent toward dye: preparation and modeling. *Bioresource Technology* **121**, 212–220.

Mohan, D. & Singh, K. P. 2002 Single- and multi-component adsorption of cadmium and zinc using activated carbon

derived from bagasse – an agricultural waste. *Water Research* **36** (9), 2304–2318.

Parab, H. & Sudersanan, M. 2010 Engineering a lignocellulosic biosorbent – coir pith for removal of cesium from aqueous solutions: equilibrium and kinetic studies. *Water Research* **44** (3), 854–860.

Qu, J. J., Song, T., Liang, J. S., Bai, X., Li, Y., Wei, Y. N., Huang, S. Q., Dong, L. Y. & Jin, Y. 2019 Adsorption of lead (II) from aqueous solution by modified *Auricularia* matrix waste: a fixed-bed column study. *Ecotoxicology and Environmental Safety* **169**, 722–729.

Rameshraja, D. & Srivastava, V. C. 2012 Quinoline adsorption onto granular activated carbon and bagasse fly ash. *Chemical Engineering Journal* **181–182** (182), 343–351.

Scott, J. A. & Karanjkar, A. M. 1998 Immobilized biofilms on granular activated carbon for removal and accumulation of heavy metals from contaminated streams. *Water Science and Technology* **38**, 197–204.

Shi, J. X., Han, Y. X., Xu, C. Y. & Han, H. J. 2019 Anaerobic bioaugmentation hydrolysis of selected nitrogen heterocyclic compound in coal gasification wastewater. *Bioresource Technology* **278**, 223–230.